



Surface flatness and roughness of diamond wire electrical discharge sawing mono-crystalline silicon with improved bath cooling

Jian Qiu^{1,2} · Xiaofei Li³ · Jianzhuang Lv² · Shanbao Zhang²

Received: 24 October 2021 / Accepted: 28 March 2022 / Published online: 7 April 2022
© The Author(s), under exclusive licence to Springer-Verlag London Ltd., part of Springer Nature 2022

Abstract

The cooling method of silicon material sawing in solar energy industry is jet cooling and flood cooling. In this paper, a machining method of diamond wire electrical discharge sawing (DWEDS) under environmentally improved bath cooling was proposed. Its advantages were compared to jet cooling by carrying a series of sawing tests. It was found that DWEDS under bath cooling obtained better machining accuracy and better surface quality than that under jet cooling. Also, the machining accuracy and cutting efficiency in DWEDS were better than those in diamond wire sawing (DWS). The same conclusions were proved by scanning electron microscope observation of the wafer surface. In addition, the wire tension in DWEDS sawing was found more stable than that in DWS. Finally, the wire wear was as another indicator to evaluate the cooling effect. No significant difference in wire wear between bath cooling and jet cooling was found. However, the wire wear of DWEDS under the same cooling method is higher than that of DWS, which means the discharge effect is helpful to the wire self-sharpening from another point of view.

Keywords DWEDS · Bath cooling · Jet cooling · Surface roughness · Surface flatness · Wire wear

1 Introduction

Mono-crystalline silicon ingots are produced by the Czochralski (Cz) process. Mono-crystalline silicon wafers for photovoltaic solar cells are manufactured by wire sawing processes. In recent years, loose abrasive slurry wire sawing (LAS) has been replaced by fixed abrasive diamond wire sawing (DWS) [1]. In the LAS processing, loose SiC particles are involved in a polyethylene glycol-based slurry poured onto a stainless steel wire web to cut silicon by the action of free abrasive grinding. Also, the coolant is the slurry. In the DWS processing, diamond grains fixed to the steel wire with electroplated nickel are used to saw silicon material, and a water-based cutting fluid is used [2]. Although the two-body grinding of DWS has the advantages

of cutting efficiency, wire wear [3], and environmental pollution [4] compared with the three-body grinding of LAS. However, the amount of cutting fluid is still huge. At present, the cooling methods of silicon wire sawing in photovoltaic industry are jet cooling and flood cooling [5]. Due to the huge flow of jet or flood, great consumption of cutting fluid are met, which greatly presents the problem of cutting fluid recycling, processing cost, and environmental pollution [6, 7]. And the impact of coolant spray forms water mist, which poses a great challenge to the sealing of spindle and harm to human body. Similar to the large flow of flooding cooling, high-pressure cooling is also a cooling method by increasing flow and pressure, which can ensure the fluid entering the cutting zone [8]. However, high-pressure fluid cooling is not conducive to the stability of the wire web in the wire sawing process.

In the field of hard and brittle material machining such as silicon wire sawing, few studies on cooling and lubrication were found. Goel et al. [9] used distilled water as a preferred coolant on diamond turning of single crystal 6H-SiC on an ultra-precision diamond turning machine in order to improve the tribological performance and found surface finish of $R_a = 9.2$ nm which is better than any previously reported value on SiC. Li et al. [10] found oil coolant could

✉ Jian Qiu
qiu1981@163.com

¹ School of Mechanical Engineering, Qingdao University of Technology, Qingdao 266520, China

² Research and Development Centre, Qingdao Gaoce Technology Co., Ltd., Qingdao 266114, China

³ Research and Development Centre, Qingdao GermanLitho Co., Ltd., Qingdao 266109, China

effectively increase the thermal diffusivity and decrease the friction coefficient between cutting tools and KDP crystals, and decrease the cutting temperature during fly-cutting by 9.42–36.70% compared with that in dry cutting process. Little research on the cooling effect could be found in the field of photovoltaic wire sawing, but rich experience in the research on the cutting performance of the fluid type, cooling parameters, and flow of coolant in the field of metal cutting could be provided. Under the background of environmental protection and sustainable development, minimum quantity lubrication (MQL) and other less coolant free processing methods were paid more attention in the field of metal cutting. Cooling methods such as cryogenic, hybrid, and vegetable fluid were present in many researches [11, 12]. Khatri and Jahan [13] found tool wear mechanisms during milling of titanium alloy Ti-6Al-4 V under MQL cooling conditions are different with that in dry, flood coolant conditions with the same cutting parameters. Liu et al. [11] found blended coolant for MQL by leveraging the mutual solubility of castor oil and ethanol has advantages on the reductions of vibration intensity, tool wear, and surface hardness in turning AISI 304 steel comparing to dry, flood cutting, and vegetableoil MQL and 95% ethanol MQL. Khanna et al. [14] found the performance of sustainable cryogenic machining is superior in terms of tool wear, power consumption, and subsurface microhardness while the better surface finish for the flood machining. Prassan et al. [15] showed cryogenic LN₂ and LCO₂ as cooling and lubrication could reduce tool wear and power consumption, and improve machining productivity and quality in drilling titanium alloy compared with cooling and lubrication techniques as dry, flood cooling. Nanofluid is another technique to improve machining performance by cooling and lubrication. Ghasemi et al. [16] investigated the effect of using nanofluid as a coolant on heat dissipation from electronic components and found it enhanced heat transfer performance.

When evaluating the performance of cooling and lubrication, tool life and wear [8], machining accuracy, surface quality and integrity [8, 15], machining state, chip formation [17], residual stress, and energy consumption [15] are generally used as an evaluation indicators. Also, cutting vibration [14], cutting temperature, and force [17] were focused on to evaluate cutting performance. Rajaguru [18] evaluated the cutting performance of super duplex stainless steels under dry, flood, and MQL using the machinability indicators such as tool wear, cutting force, surface finish, morphology of chips, and residual stress. Kaynak [19] selected tool wear rate, force components, chip breaking, surface topography, dimensional accuracy, microhardness, and XRD analysis as machining performance measures to assess the machining performance of Ti-5553 alloy by utilizing high pressure coolant delivery, MQL, and flood

cooling. Gueli et al. [20] used the indicators of cumulative tool wear, cutting forces, surface roughness, topography, burr formation, and chip morphology to compare the performance of dry and flood coolant machining Inconel 718 using uncoated carbide tools. Race et al. [21] measured and compared tool wear, surface roughness, residual stress, and energy consumption to study the performance of low-impact cooling strategies as dry milling or MQL in the machining of SA516 steel.

In the field of crystalline silicon wire sawing, the contact area between diamond wire and processed materials is large due to the huge cutting density. Cooling and lubrication methods such as MQL obviously cannot meet the requirement. Most processes used in the metal cutting could not perform its cooling and lubricating properties. In this research, the application of bath cooling method was proved better on machining accuracy and surface quality [22]. It was found that the machining surface roughness corresponding to bath sawing is better than that of jet sawing. In this paper, a DWEDS method using bath cooling is proposed. It is focused on the flatness reflecting machining surface accuracy and compares the advantages of bath sawing with jet sawing. By comparing the flatness and roughness of sawn surface, the advantages of DWEDS under bath cooling are obtained. In addition, the results of flatness and roughness obtained by DWEDS machining silicon wafer under jet cooling are compared with those of DWS. In addition, surface topography, wire tension, and wire wear are selected as the other evaluation indicators.

2 Materials and method

2.1 Cooling method

The cooling method of bath sawing with a water tank is shown in Fig. 1a and compared with jet cooling as shown in Fig. 1b. The advantages of bath cooling is that the diamond wire can be fully cooled and more cutting fluid can be immersed in the sawing kerf to ensure sufficient cooling and lubrication. Meanwhile, the carrying effect of diamond wire on cutting fluid can bring more fluid into the cutting zone. In addition, the cutting fluid injected into the water tank to form a stable fluid pool improves the disturbance of fluid on the diamond wire by the direct injection method. Thus, the wire tension fluctuation of diamond wire is improved. Compared with jet cooling, bath cooling keeps more cutting fluid in the water tank without considering more fluid splash loss. Therefore, the amount of cutting fluid can be greatly reduced, which is beneficial to environmental protection.

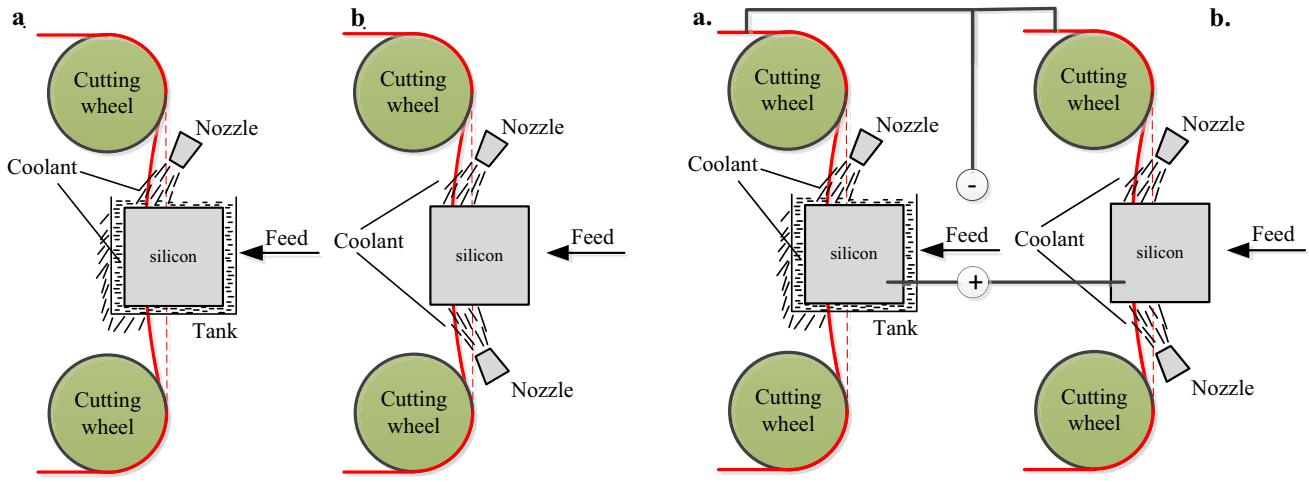


Fig. 1 Principle of bath sawing comparing with jet sawing (**a** bath cooling condition with nozzle and water tank; **b** jet cooling condition with nozzle)

2.2 Diamond wire electrical discharge sawing method

The diamond wire electrical discharge sawing is defined as a compound sawing method. The diamond wire is used as negative electrode, and a pulse voltage is added between the wire electrode and the positive workpiece electrode, the simplified discharge circuit as shown in Fig. 2. At the moment of electrical discharge breakdown of the inter medium between the electrodes, a large amount of heat energy is released to melt and gasify the material on the surface of workpiece. Meanwhile, the diamond grain easily cuts the soft materials and removes it into chips than the DWS without material melt. With the explosion of inter medium between electrodes, the silicon materials on the surface of workpiece are brought out for erosion. Then, the discharge pits are formed to achieve the purpose of processing.

2.3 Determination and definition of evaluation indicators

2.3.1 Machining process signal

The wire tension is the key parameter to evaluate the machining process. The value and fluctuation of wire tension in the cutting process can reflect the load action on the diamond wire. If the load is small, it means that the material is easy to remove. If the tension stability is high, it means that the cutting process is stable.

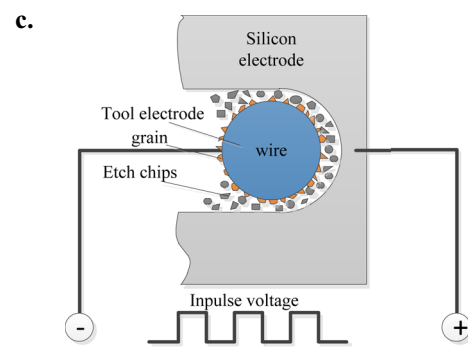


Fig. 2 Principle of diamond wire electrical discharge sawing (**a** DWEDS bath sawing; **b** DWEDS jet sawing; **c** simplified circuit of electrical discharge)

2.3.2 Flatness

The machining accuracy of silicon wafer is usually evaluated by TTV [23], bow [24], warp [25], and other indicators. In the final analysis, it is the evaluation of surface flatness

Table 1 Specifications of machine tool and the information of silicon ingot and diamond wire

Properties	Specifications
Worktable size	470 mm × 710 mm
Worktable elevation	350 mm × 450 mm
Maximum cutting thickness	400 mm
Discharge current	2–11 A
Discharge voltage	100 V
Coolant	Water
Wire diameter	0.175 mm
Maximum wire tension	40 N
Resistivity of diamond wire	(2.16–2.32)E-07
Thickness of silicon workpiece	50 mm
Resistivity of mono-crystalline silicon	0.24 Ω cm

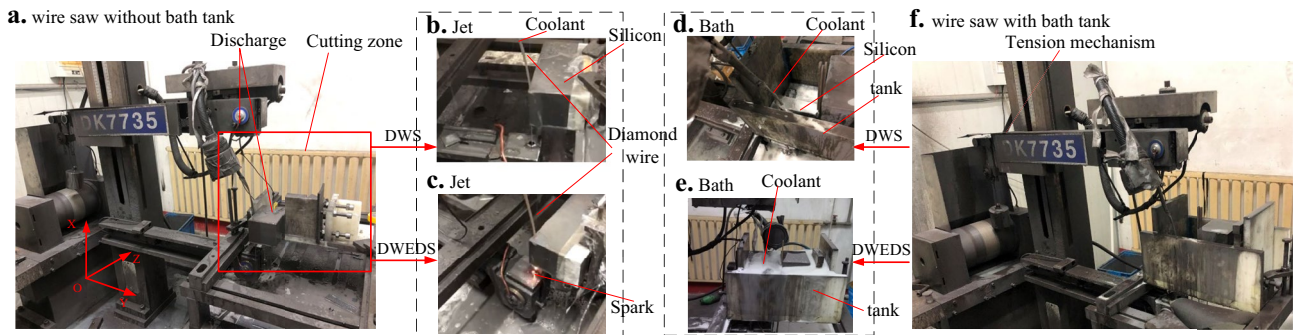


Fig. 3 Sawing test of DWEDS with improved bath cooling (**a** wire sawing based on jet cooling; **b** DWS with jet cooling; **c** DWEDS with jet cooling; **d** DWS with bath cooling; **e** DWEDS with bath cooling; **f** wire sawing based on bath cooling)

and thickness. For the evaluation of machining accuracy in single wire sawing, the evaluation indicators of wafer thickness such as TTV, bow, and warp are not suitable. Thus, the flatness is used to evaluate the accuracy of a single machining surface.

The flatness of sawing surface is defined as the minimum zone of the real machining plane relative to the ideal plane. The real plane exists in the form of numerical values obtained from multiple measuring points in the actual measurement. The ideal plane has geometric significance in theory [26, 27]. The minimum zone of flatness is defined as the zone between two parallel planes that can contain the real plane and have the minimum width.

The calculation methods of flatness mainly include methods of minimum zone of flatness, least square plane, diagonal plane, and three point plane. In this paper, the least square plane method was used to calculate and evaluate the flatness of the processed silicon wafer surface. It is defined as the method taking the least squares mean plane as the evaluation base to obtain the flatness. The least squares mean plane is an ideal plane that minimizes the sum of squares of the distances from each point on the real plane to the ideal plane.

$$f_{is} = D_{max} - D_{min} \tag{1}$$

where D_{max} and D_{min} are the maximum and minimum deviation values of the measuring points from the least squares mean plane. D_i takes a positive value above least squares mean plane and a negative value below least squares mean plane; i is the number of measuring points.

2.3.3 Surface roughness

The arithmetic mean deviation Ra of the surface profile, the maximum height Rz of the surface profile, the root mean square Rq of the surface profile, and the mean width Rsm of the surface profile elements are recommended to characterize the surface roughness of silicon wafer [28–30]. The evaluation indicators are defined in standards ISO1302 [31] and ISO4287 [32].

Arithmetical mean deviation of the sawing surface profile

Ra is the arithmetic mean of absolute value of sawing surface profile offset within sampling length l , as shown in Eq. (2).

$$Ra = \frac{1}{l} \int_0^l |Z(x)| dx \tag{2}$$

where l is sampling length of the sawing surface profile.

Table 2 Machining accuracy comparison test between jet cooling and bath cooling during DWEDS

No	Feed speed, $\mu\text{m/s}$	Pulse on-time t_{on} , μs	Pulse off-time $t_{off} \times t_{on}$, μs	Power	Method
1: 1–5	50	50, 60, 70, 80, 90	3	3	bath
1: 6–10	50	50, 60, 70, 80, 90	4	3	bath
1: 11–15	50	50, 60, 70, 80, 90	5	3	bath
2: 1–5	50	50, 60, 70, 80, 90	3	3	jet
2: 6–10	50	50, 60, 70, 80, 90	4	3	jet
2: 11–15	50	50, 60, 70, 80, 90	5	3	jet

Table 3 Machining accuracy comparison test between DWEDS sawing and DWS sawing using bath cooling

No	Feed speed, $\mu\text{m/s}$	Pulse on-time $t_{\text{on}}, \mu\text{s}$	Pulse off-time $t_{\text{off}}, \times t_{\text{on}}, \mu\text{s}$	Power	Method
3: 1–6	30, 40, 50, 60, 70, 80	70	3	3	DWEDS
4: 1–6	30, 40, 50, 60, 70, 80	-	-	-	DWS

Skewness of the sawing surface profile R_{sk} is the measure of the asymmetry of the probability density function of the ordinate values, which is the quotient of the mean cube value of the ordinate values $Z(x)$ and the cube of R_q within a sampling length. The equation is shown in Eq. (3).

$$R_{sk} = \frac{1}{R_q^3} \left[\frac{1}{l} \int_0^l Z^3(x) dx \right] \tag{3}$$

where R_q is the root mean square value of the ordinate values $Z(x)$ within a sampling length.

Kurtosis of the sawing surface profile R_{ku} is the measure of the sharpness of the probability density function of the ordinate values, which is the quotient of the mean quartic value of the ordinate values $Z(x)$ and the fourth of R_q within a sampling length. The equation is shown in Eq. (4).

$$R_{ku} = \frac{1}{R_q^4} \left[\frac{1}{l} \int_0^l Z^4(x) dx \right] \tag{4}$$

Mean width of the sawing surface profile elements R_{sm} is the mean value of the profile element widths X_s within a sampling length, as shown in Eq. (5).

$$R_{sm} = \frac{1}{m} \sum_{i=1}^m X_{s_i} \tag{5}$$

Table 4 Machining accuracy comparison test between DWEDS sawing and DWS sawing using jet cooling

No	Feed speed, $\mu\text{m/s}$	Pulse on-time $t_{\text{on}}, \mu\text{s}$	Pulse off-time $t_{\text{off}}, \times t_{\text{on}}, \mu\text{s}$	Power	Method
5: 1–6	30, 40, 50, 60, 70, 80	70	3	3	DWEDS
6: 1–6	30, 40, 50, 60, 70, 80	-	-	-	DWS

where X_{Si} is the spacing distance between each adjacent local peaks; $i + 1$ is the total number of acquired local peaks.

3 Experiments

3.1 Experimental set-up

The sawing test was carried out on an improved DK7735 wire sawing machine tool with specifications as shown in Table 1. The machine tool had been reformed on the electrical discharge mechanism and tension mechanism. The experimental set-up is shown in Fig. 3. Two nozzles were used in the jet cooling to cool the cutting zone, as shown in Fig. 3b, c. The bath cooling was realized using a water tank with small amount fluid injecting into the tank, as shown in Fig. 3d, e. The cooling medium in the test was water. Mono-crystalline silicon with resistivity $0.24 \Omega \text{ cm}$ was used as the workpiece electrode and diamond wire with diameter of 0.175 mm was used as tool electrode. The resistivity of mono-crystalline silicon was measured by KINGSUN silicon material tester.

3.2 Cutting test design

In the sawing verification test, the size of mono-crystalline silicon workpiece was $105 \text{ mm} \times 62 \text{ mm} \times 70 \text{ mm}$. The sawing parameters of sawing test for machining accuracy comparison test between jet cooling and bath cooling during DWEDS are shown in Table 2. In the test, the wire shall be replaced once in each group of test in order to ensure the accuracy of the test data, and then another group of tests shall be carried out after changing a new wire. The cooling parameters selected in the test are fixed values, with a maximum flow rate of 50 L/h .

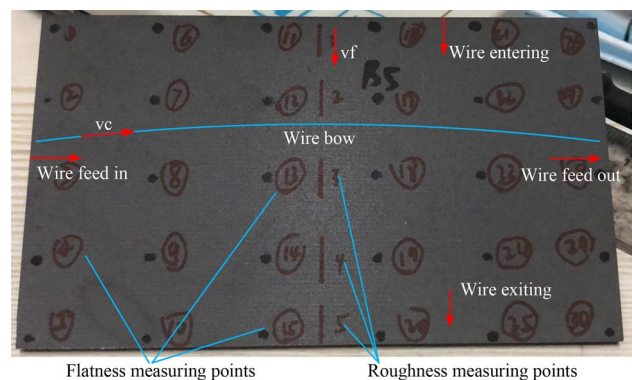


Fig. 4 Measuring points for evaluation of flatness and roughness

Fig. 5 Tension comparison between jet cooling and bath cooling during DWEDS (**a** $v_f=50$, $t_{on}=70$, $t_{off}=3$, $P=3$; **b** $v_f=50$, $t_{on}=90$, $t_{off}=4$, $P=3$; **c** $v_f=50$, $t_{on}=60$, $t_{off}=5$, $P=3$)

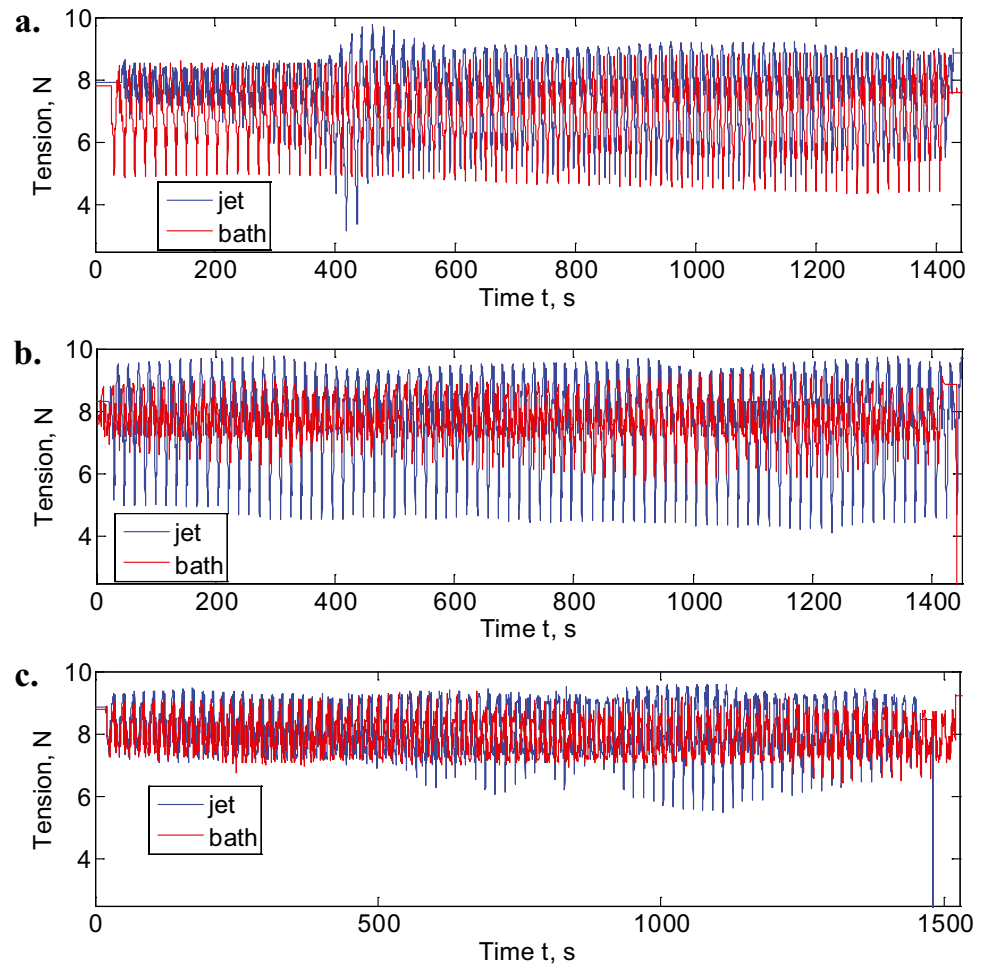


Fig. 6 Tension comparison between DWEDS and DWS with bath cooling (**a** feed speed $40 \mu\text{m/s}$, power 3, $t_{off}=3 \times t_{on}$; **b** $80 \mu\text{m/s}$, power 3, $t_{off}=3 \times t_{on}$)

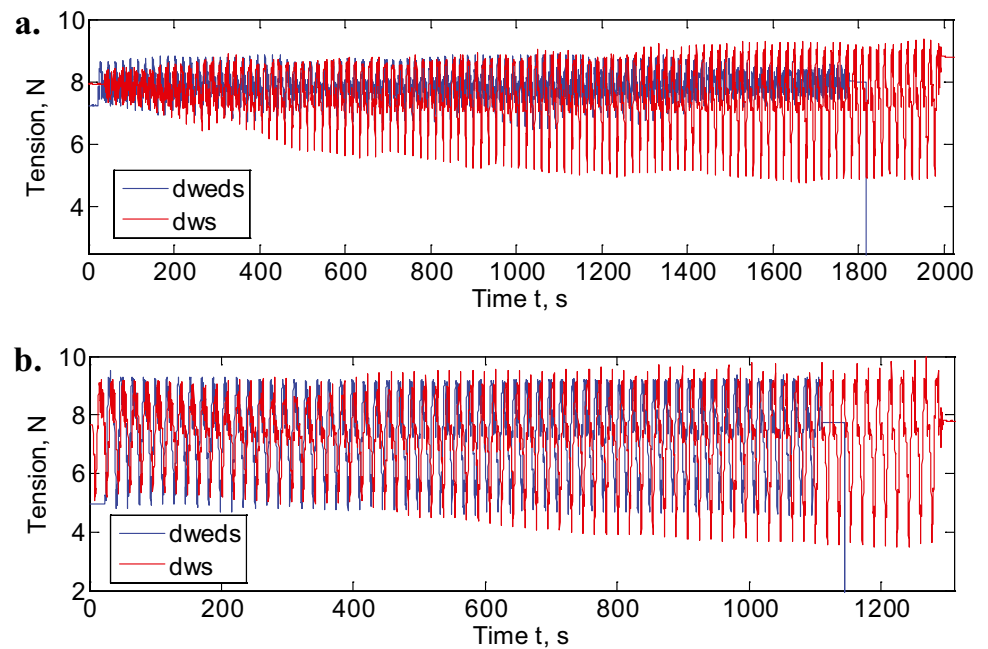


Table 5 Machining time (s) comparison test between DWEDS sawing and DWS sawing using bath cooling

No	1	2	3	4	5	6
DWS	2531.8	1976.6	1655.7	1446.7	1282.8	1185.7
DWEDS	2292.4	1752.9	1426.6	1239.6	1086.3	993.5
Ratio	9.46%	11.32%	13.84%	14.32%	15.32%	16.21%

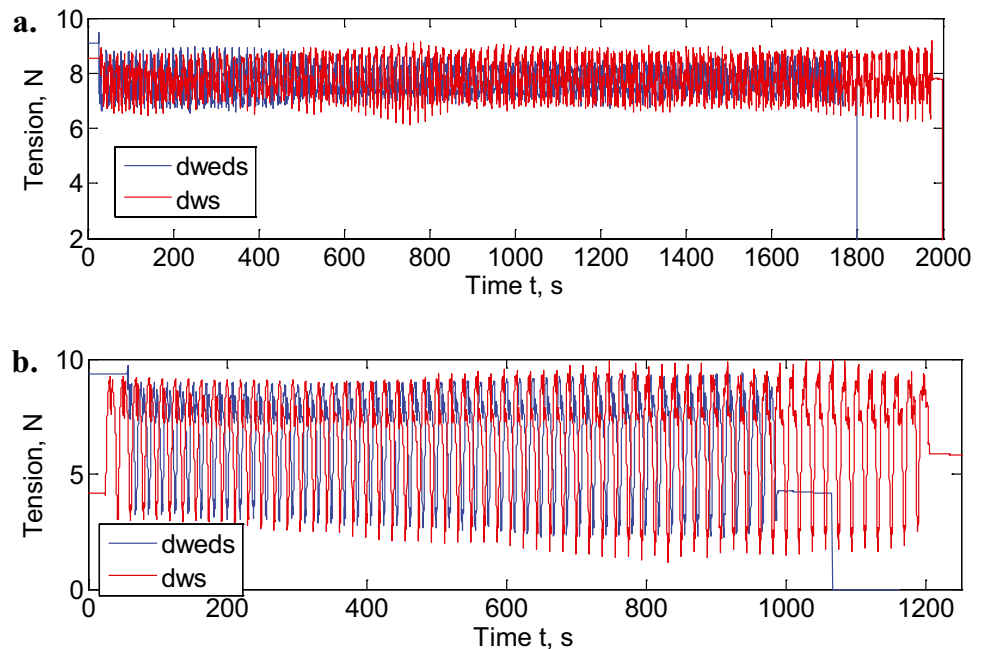
A series of sawing tests were designed to compare the machining accuracy and surface roughness between DWEDS sawing and DWS sawing under bath cooling condition. The sawing parameters are shown in Table 3. Similarly, experiments with the same sawing parameters under jet cooling conditions were also used to compare the machining advantages of DWEDS to DWS, as shown in Table 4.

3.3 Measurement

The flatness of silicon wafer surface was measured by Mitutoyo Dial Indicator with measuring accuracy 1 μm, model ID-C112X. In the test, the number of measuring points for the flatness evaluation of wafer was 5 × 6 according to the length and width directions, respectively. There were 30 measuring points on a silicon wafer surface, as shown in Fig. 4. For the flatness of a surface, it is calculated from the 30 measuring points and outputs one flatness value.

The surface roughness of silicon wafer was measured by Mitutoyo SJ210 Surface Profiler. The surface roughness was measured according to the center line of silicon wafer in the feeding direction of diamond wire, which was divided into 5 measuring points, as shown in Fig. 4. For a surface, 5 roughness values are output. The surface quality was combined with Hitachi TM3030Plus Scanning Electron Microscope (SEM) for evaluation.

Fig. 7 Tension comparison between DWEDS and DWS with jet cooling (a feed speed 40 μm/s, power 3, $t_{off}=3 \times t_{on}$; b 80 μm/s, power 3, $t_{off}=3 \times t_{on}$)



A self-made tension testing mechanism was adopted for the wire tension test in the sawing process, and the strain type tension sensor was installed. The measuring range is 0–100 N, the linearity is $\leq 3\%$, and the repetition error is 3% . RS485 is adopted for signal communication.

4 Results and discussion

4.1 Wire tension and cutting efficiency

The tension mechanism used in this research is a weight tension mechanism, which can ensure the constant tension on the diamond wire in the sawing process. The tension comparison results of several groups of typical parameters in the test are listed in order to understand the change of tension on diamond wire during sawing, as shown in Fig. 5. In Fig. 5a, the wire tension stability of bath cooling is better than that of jet cooling, and there is no obvious change in the tension during the whole sawing process with bath cooling. In Fig. 5b, the tension in jet cooling and bath cooling is stable, but the tension envelope of bath cooling is significantly smaller than that of jet cooling, indicating that the tension value is more concentrated and the stability is better. In Fig. 5c, the wire tension stability, tension envelope, and processing process in bath cooling are obviously better than

Table 6 Machining time comparison test between DWEDS sawing and DWS sawing using bath cooling

No	1	2	3	4	5	6
DWS	2457.1	1950.4	1631.6	1393.2	1379.5	1178.8
DWEDS	2207.7	1741.1	1391	1101.2	1002.4	921.7
Ratio	10.15%	10.73%	14.75%	20.96%	27.34%	21.81%

jet cooling. In addition, the processing time of each group of data under the same sawing parameters in DWEDS using jet cooling and bath cooling are the same.

The processing time of DWEDS is significantly shorter than that of DWS. Two optional groups of data are shown in Fig. 6. Under the condition with the same feed rate, the theoretical sawing time is the same. The main factor causing the difference in the actual sawing time between DWEDS and DWS is wire bow, which shows that the wire bow of DWS is larger than that of DWEDS. It shows that DWEDS has a significant effect on improving the wire bow and reducing the macro force during wire sawing process. And the cutting efficiency caused by the reduction of wire bow is reduced by 9.46–16.21% in the six groups of comparative data, as the statistics shown in Table 5. The faster the feed, the greater the improvement of cutting efficiency.

When jet is used for both DWS and DWEDS, the same conclusion can be drawn as the use of bath cooling, as two optional groups of data shown in Fig. 7, the processing time of DWEDS is significantly shorter than that of DWS, and the efficiency is improved from 10.15 to 27.34%. Almost the faster the feed, the greater the improving ratio, as shown in Table 6. The wire tension stability of DWEDS is significantly improved compared with DWS.

4.2 Machining surface flatness

Figure 8 shows the comparison between the DWEDS machining accuracy obtained by using bath cooling and that obtained by using traditional jet cooling corresponding to the parameters in Table 2. It can be found that the accuracy of jet cooling and bath cooling is different under the same sawing conditions. Except for the 1st group of parameters,

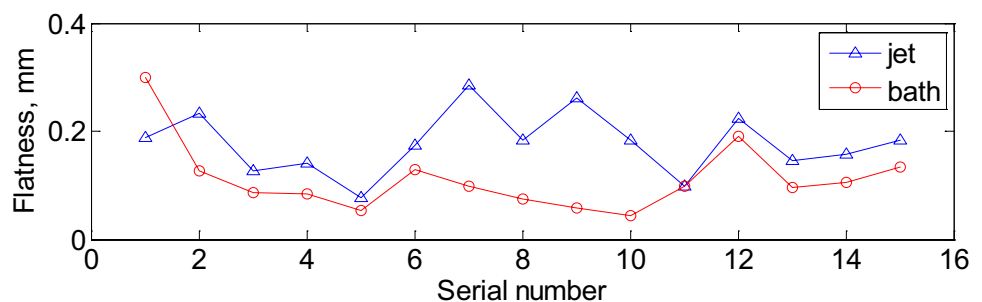
the machining surface accuracy corresponding to most parameters is higher under bath cooling conditions. When the pulse off-time is 4 times of pulse on-time, the machining accuracy corresponding to bath cooling with on-time of 60, 70, 80, and 90 μ s is obviously better than jet cooling.

Figure 9 shows the contour height distribution on the surface of the group tests of 1–4 and 2–4 in Table 2 with the two processing methods. It can be seen that the consistency of the surface height distribution of bath saving is obviously better than that of jet saving, and the linear distribution of flatness distribution based on the least square plane method is more concentrated.

For the comparison between the two wire sawing methods using bath cooling as shown in Fig. 10, corresponding to the parameters in Table 3, it can be found that the machining accuracy of wafer surface obtained by DWEDS under bath cooling is better than that of DWS. With the increase of feed speed, the flatness of DWEDS does not change obviously. The accuracy difference is the most significant when the feed speed is 60, 70, and 80 μ m/s.

Figure 11 shows the contour height distribution on the surface of the group tests of 3–4 and 4–4 in Table 3 in the processing of DWEDS and DWS. It can be seen that the consistency of the surface height distribution of DWEDS is obviously better than that of DWS, and the linear distribution of flatness distribution based on the least square plane method is more concentrated.

For the two wire sawing methods using jet cooling, corresponding to the parameters in Table 4, the flatness of DWEDS is not as good as DWS after the feed speed exceeds 40 μ m/s, as shown in Fig. 12. Combined with the results of bath cooling of DWEDS and DWS as shown in Fig. 10, it shows that when the feed rate exceeds 40 μ m/s, the machining accuracy obtained by jet cooling is not as good as that obtained by bath cooling.

Fig. 8 Machining accuracy comparison between jet cooling and bath cooling during DWEDS

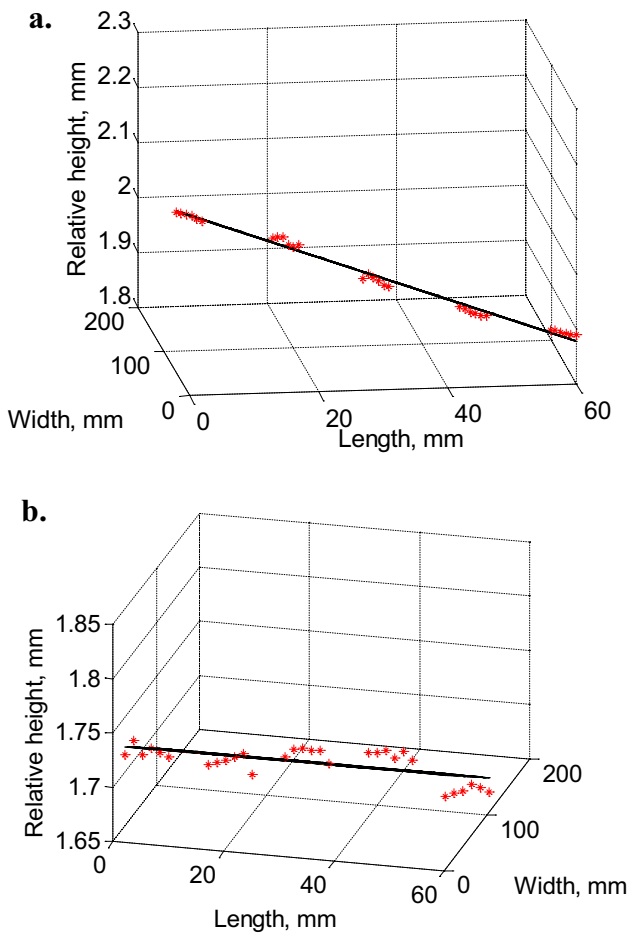


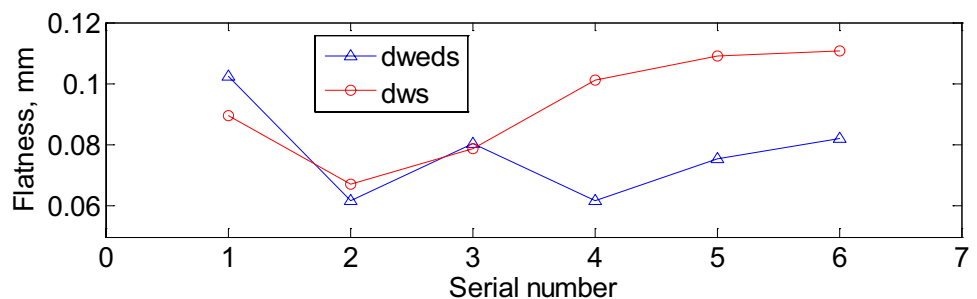
Fig. 9 Surface relative height distribution at feed speed 50 $\mu\text{m/s}$, pulse on-time 80 μs , pulse off-time 240 μs , and power 3 (a bath sawing; b jet sawing)

4.3 Surface roughness

4.3.1 Bath cooling and jet cooling in DWEDS

Figure 13a shows the surface roughness Ra distribution of silicon wafer obtained by DWEDS under bath cooling and jet cooling conditions. Every five measuring points are a measuring group of one silicon wafer surface, corresponding

Fig. 10 Machining accuracy comparison between DWEDS sawing and DWS sawing using bath cooling



to five positions evenly distributed from wire entering to wire exiting along the center line of the silicon wafer in the wire feeding direction. Every five silicon wafers correspond to a pulse off-time t_{off} parameter. When pulse off-time is 3 times of pulse on-time t_{on} , the corresponding surface roughness of silicon wafer increases with the increase of pulse on-time t_{on} from 50 μs to 90 μs . The same trend is reproduced in each of the five variable pulse on-time tests with pulse off-time $4 \times t_{\text{on}}$ and pulse off-time $5 \times t_{\text{on}}$, in which the abnormal data of jet cooling at pulse on-time 60 μs and pulse off-time $4 \times t_{\text{on}}$ is discharged. The increase of pulse on-time is helpful to improve the discharge effect, but it is not conducive to obtain better surface roughness.

For a single silicon wafer, the roughness at the middle position of silicon wafer profile is lower than that of the wire entering and wire exiting positions. It can be understood that the discharge effect at the middle position of wafer is weak, indicating that a better cooling condition is helpful to enhance the discharge effect of DWEDS.

Comparing the three processing conditions of pulse off-time $3 \times t_{\text{on}}$, $4 \times t_{\text{on}}$ and $5 \times t_{\text{on}}$, it can be seen that the roughness corresponding to larger pulse off-time $5 \times t_{\text{on}}$ is the best with smaller roughness difference between each measuring point on one silicon wafer surface.

In Fig. 13a, the roughness of the machined surface cooled by bath cooling is slightly better than that cooled by jet cooling, and the fluctuation of roughness is also smaller. The same conclusion can be drawn from the distribution of skewness coefficient Rsk (Fig. 13b) and kurtosis coefficient Rku (Fig. 13c) on the surfaces of and. Both of the kurtosis coefficient and skewness coefficient fluctuate less during bath cooling.

In addition, from the comparison of the mean width of profile element Rsm (Fig. 13d), it can be found that the mean width of profile corresponding to bath cooling is less than that corresponding to jet cooling, indicating that the surface uniformity within the sampling length is better when bath cooling is used.

At the third measuring point (the central position of the surface) of the first set of parameters in Table 2, the average surface roughness Ra obtained by the two cooling methods has little difference as shown in Fig. 13. However, in the

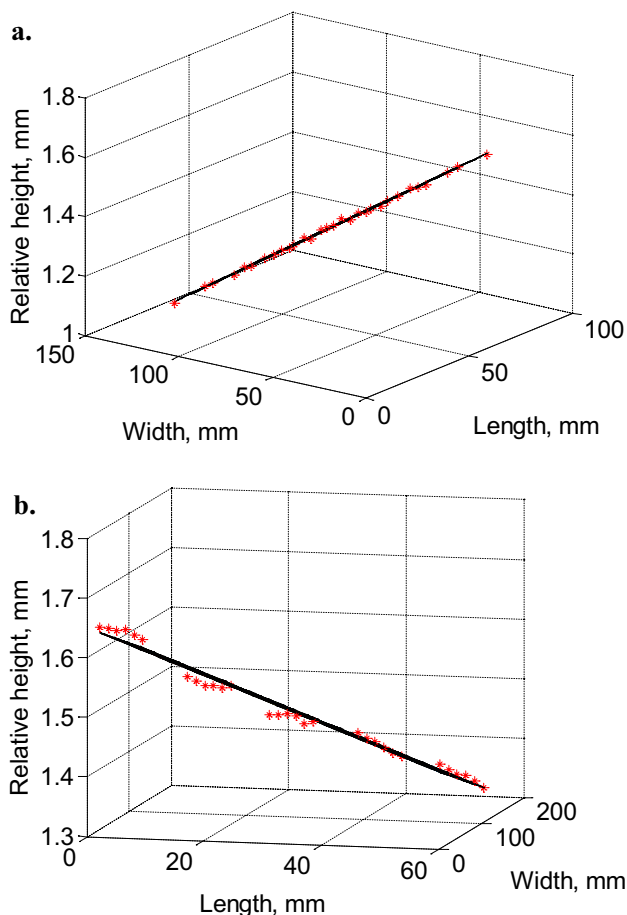


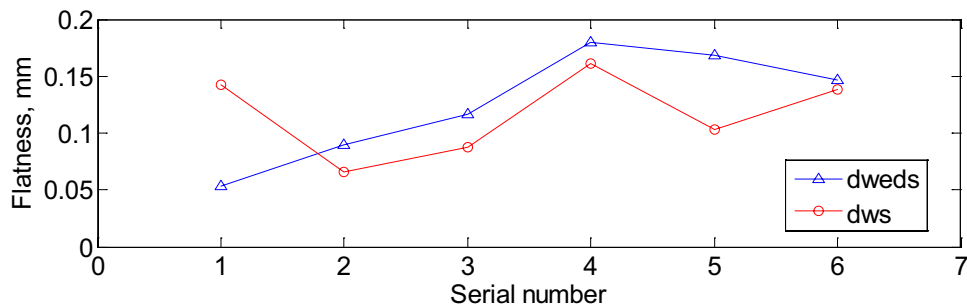
Fig. 11 Surface relative height distribution at feed speed $60 \mu\text{m/s}$, pulse on-time $70 \mu\text{s}$, pulse off-time $210 \mu\text{s}$, and power 3 (a) DWEDS; (b) DWS)

height distribution of the surface profile, the surface profile of bath sawing is more uniform and periodic, while surface profile of jet sawing fluctuates violently and shows poor regularity, as shown in Fig. 14.

4.3.2 DWEDS and DWS with bath cooling

The statistics of surface roughness R_a obtained under the same parameters by DWEDS and DWS with bath cooling

Fig. 12 Machining accuracy comparison between DWEDS sawing and DWS sawing using jet cooling



are shown in Fig. 15a. Every five data are the five positions on the wafer surface from wire entering to the wire exiting. The roughness of different positions on each silicon wafer surface reflects that, the roughness is the smallest when the diamond wire is cut to the middle position of silicon wafer, followed by the wire entering position, and the largest position occurs at the wire exiting position. It is found that the roughness of DWEDS machining is improved with the increase of feed speed. The inverse correlation between roughness and discharge effect of DWEDS can explain that the discharge effect is weakened. From the roughness distribution of all measuring points, it can be found that the surface roughness obtained by DWEDS is worse than that by DWS under the same bath cooling condition.

From the distribution of surface skewness coefficient R_{sk} in Fig. 15b, it can be seen that the skewness coefficient of surface roughness obtained by DWEDS is closer to the value 0 at feed speeds of $30 \mu\text{m/s}$ and $40 \mu\text{m/s}$, indicating that the micro distribution of surface peaks of DWEDS is more uniform although the average roughness is poor. The kurtosis coefficient R_{ku} of roughness is also closer to the value 3 at these two groups of feed speeds, as shown in Fig. 15c, which shows that the kurtosis distribution of profile peak of DWEDS is better than that of DWS. The roughness, profile skewness (Fig. 15b), and profile kurtosis (Fig. 15c) at feed speeds of 60, 70, and $80 \mu\text{m/s}$ have little difference between the two machining methods.

On the indicator of micro mean width of profile element, bath cooling is smaller than jet cooling, indicating that the surface uniformity within the sampling length is better, as shown in Fig. 15d.

4.3.3 DWEDS and DWS with jet cooling

As jet cooling is adopted, the surface roughness of DWEDS is significantly higher than that of DWS when the feed speed is $30 \mu\text{m/s}$ and $40 \mu\text{m/s}$. Then, when the feed speed reaches $50 \mu\text{m/s}$, the surface roughness obtained by the two machining methods is similar, as shown in Fig. 16a. From Fig. 16b, the distribution of skewness coefficient R_{sk} , it is found that the value of DWEDS is closer to 0, and the

Fig. 13 Comparison between bath cooling and jet cooling in DWEDS (a Ra; b Rsk; c Rku; d Rsm)

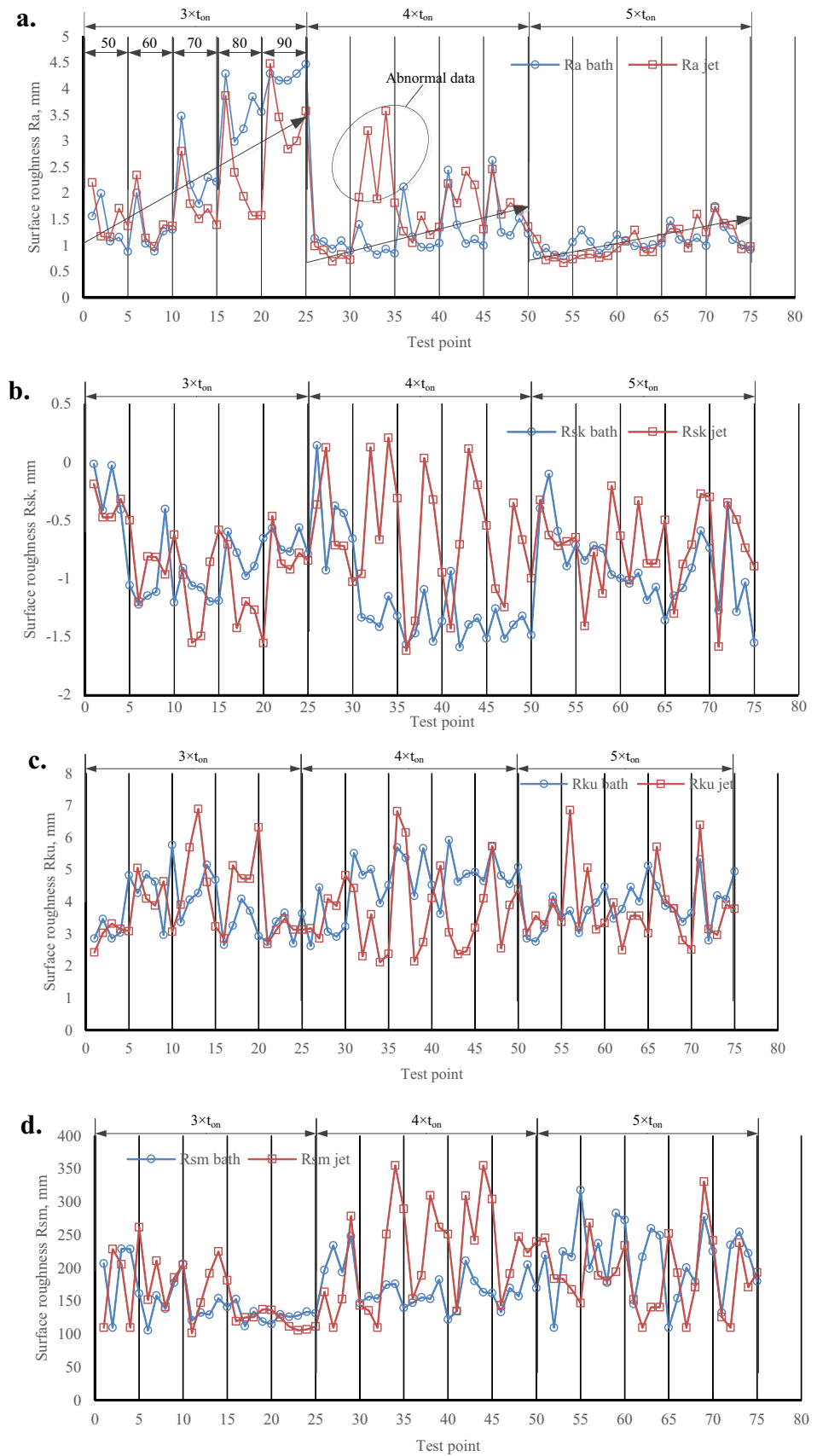
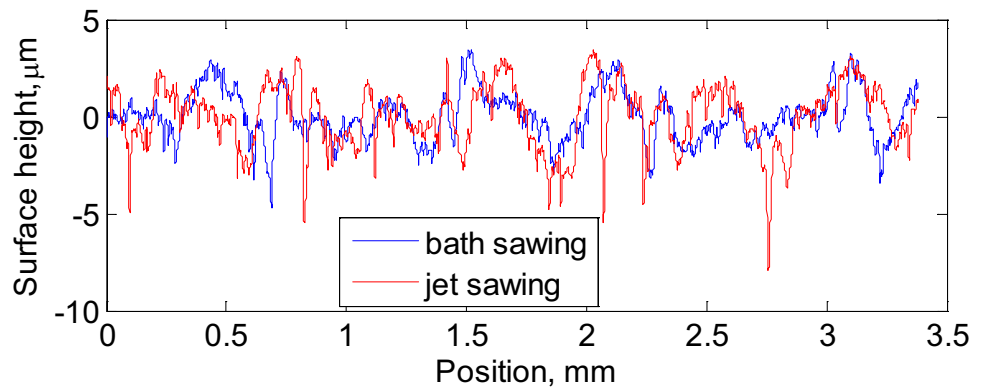


Fig. 14 Surface height comparison between bath sawing and jet sawing at feed speed $50 \mu\text{m/s}$, pulse on-time $50 \mu\text{s}$, pulse off-time $150 \mu\text{s}$, and power 3



skewness distribution of surface peak sawn by DWEDS is more uniform than that of DWS. From the kurtosis coefficient Rku in Fig. 16c, the kurtosis distribution of the machined surface of DWS is closer to 3 when the feed speed is $30 \mu\text{m/s}$, and the surface is more regular than that of DWEDS; when the feed speed gradually increases to $40 \mu\text{m/s}$ and $50 \mu\text{m/s}$, the skewness distribution of surface peak sawn by DWEDS is better than that of DWS. From the mean width of the sawing surface profile elements Rsm processed by DWEDS and DWS in Fig. 16d, it is known that the mean width of surface profile of DWEDS is more uniform than that of DWS.

4.4 Surface topography

Corresponding to the second position of wafer surface roughness at pulse on-time $60 \mu\text{s}$ and power 3 in Fig. 13 and SEM images in Table 7, little difference between the roughness under bath cooling and jet cooling is found, where the roughness of bath is slightly better, but the flatness of bath is obviously better. The roughness of bath cooling is significantly higher than that of jet cooling under the sawing with pulse on-time $80 \mu\text{s}$ and power 3, which can be proved more pits and recast defects in DWEDS than in DWS as shown in Table 7. It can also be seen from the SEM that the pits and melting recast phenomenon caused by bath discharge etching are more obvious, as shown in Table 7. Under the sawing parameters of pulse on-time $80 \mu\text{s}$ and power 4, no obvious differences in SEM and corresponding roughness are found, but the surface flatness under bath cooling is obviously better. When the pulse on-time is $70 \mu\text{s}$ and power is 5, the roughness of bath cooling and jet cooling is almost the same. Little difference between the two cooling methods is found in SEM images, but the surface flatness of bath cooling is significantly better than that of jet cooling.

From the scanning electron microscope of DWEDS and DWS processed under bath cooling as shown in Table 8, it can be seen that the discharge etching effect of DWEDS is decreasing with feed speed increasing from $30 \mu\text{m/s}$ to $50 \mu\text{m/s}$. The extent of the surface containing the characteristics of electrical discharge erosion, pits, recasting is gradually weakened, and gradually tends to produce scratches of abrasive grains. However, the surface in DWS is not obviously different, and the surface is mainly formed by the scratch of abrasive grains. Corresponding to Fig. 15, the roughness of DWEDS at feed speed $30 \mu\text{m/s}$ is significantly higher than that of DWS, while the roughness of DWEDS at feed speed $50 \mu\text{m/s}$ are equivalent to that of DWS. Although the SEM and roughness are gradually improved with the increase of feed speed, the flatness in this parameter interval does not change significantly with the change of feed speed as shown in Fig. 10. The flatness of DWEDS is significantly improved after it is higher than $50 \mu\text{m/s}$, and the results obtained by the two processing methods of roughness are the same.

4.5 Wire wear

Figure 17 shows the wire wear under the same material removal amount after 15 groups of continuous processing under the conditions of bath cooling and jet cooling. It is found from the SEM images that the wire wear under jet cooling is slightly serious than that under bath cooling, but the difference is not significant. Grains expose from both of the wires in jet cooling and bath cooling. A small amount of coating corrosion can be seen in jet cooling in b. However, the diameters of the diamond wire in the two cooling condition have no difference, no matter the diameters of wire with grains and without grains, as shown in Fig. 17a, b.

Figure 18 shows the SEM photos of the diamond wire corresponding to the same silicon material removal

Fig. 15 Comparison between DWEDS and DWS with bath cooling (**a** Ra; **b** Rsk; **c** Rku; **d** Rsm)

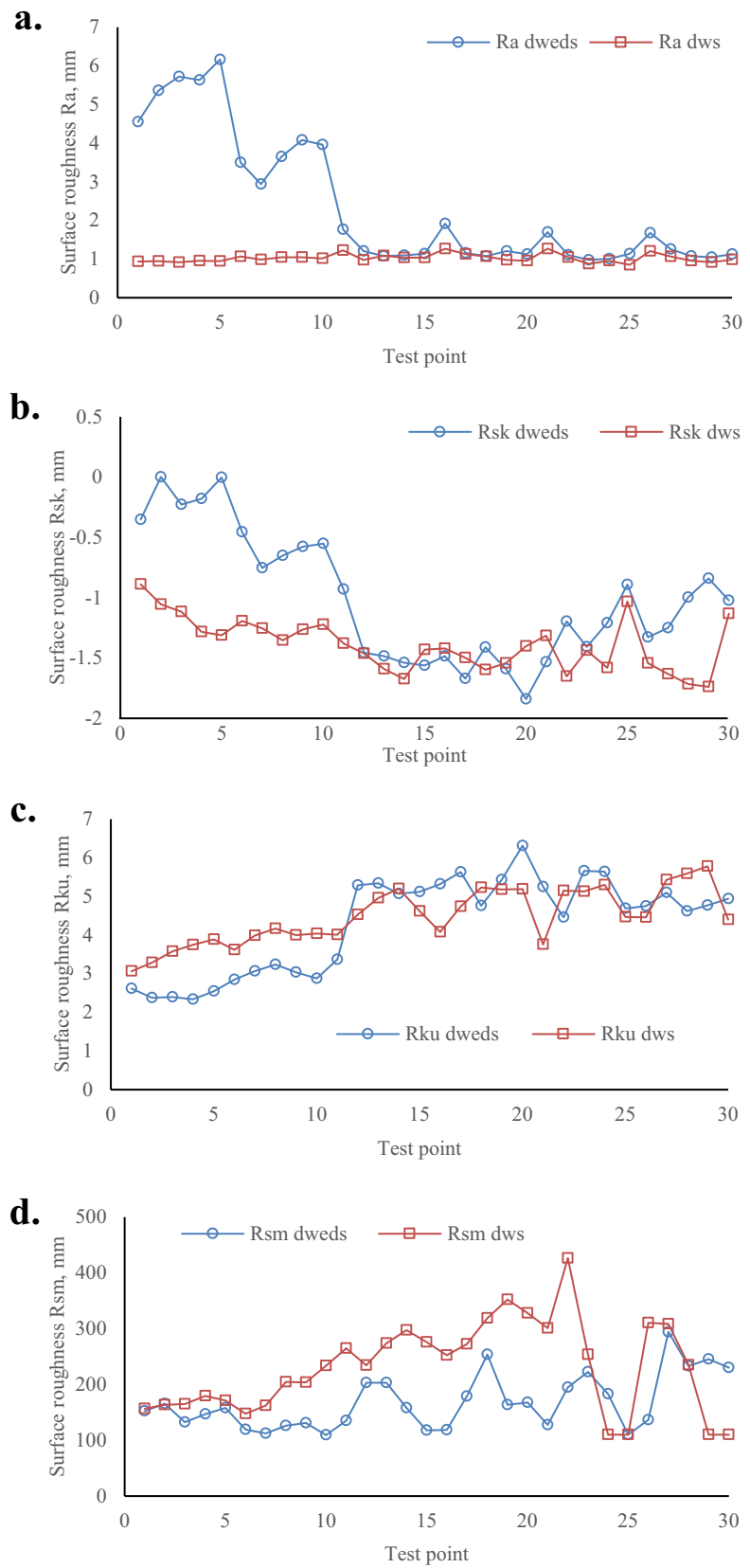


Fig. 16 Comparison between DWEDS and DWS with jet cooling (**a** Ra; **b** Rsk; **c** Rku; **d** Rsm)

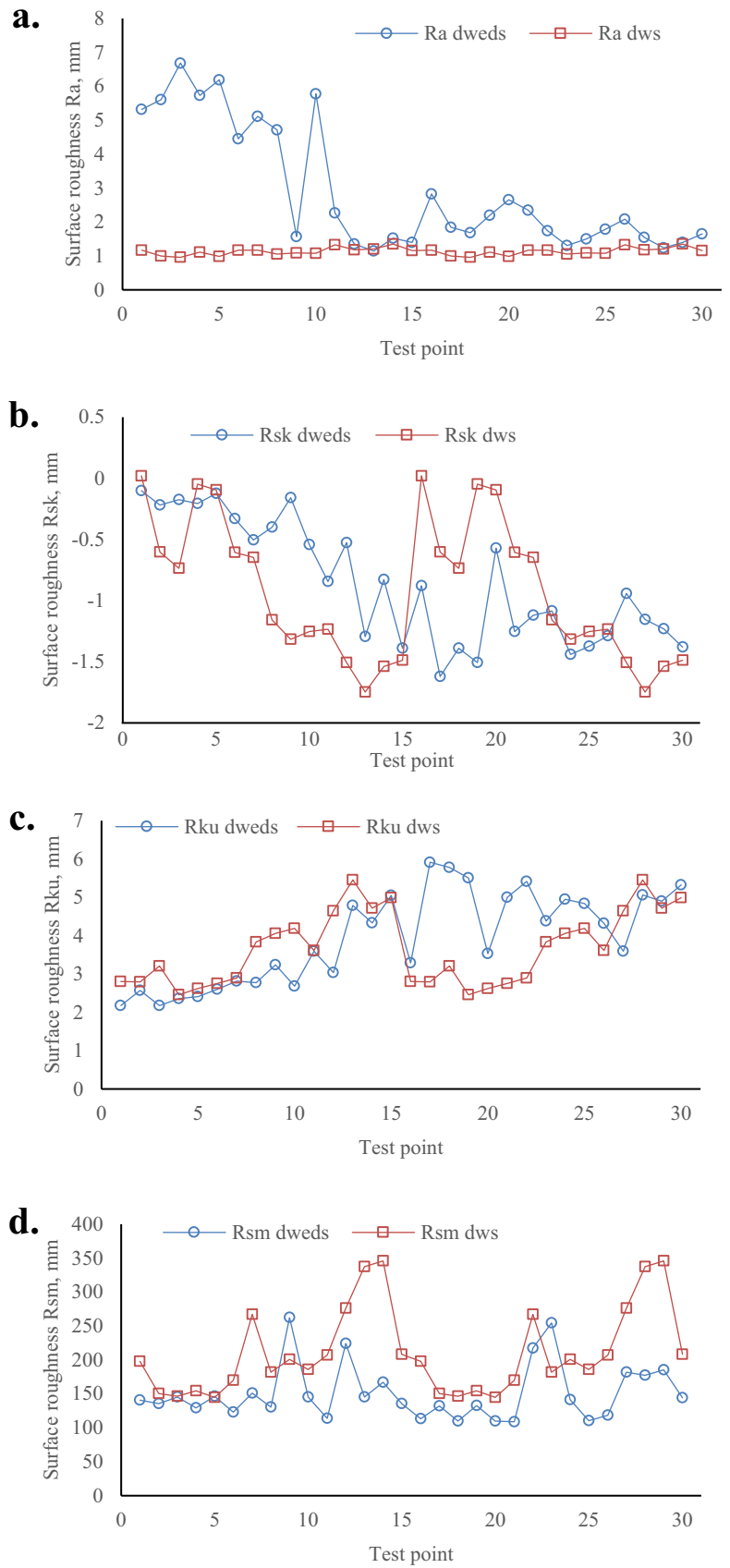
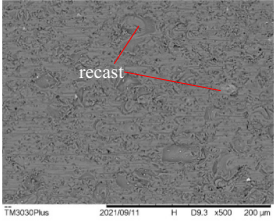
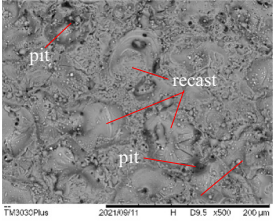
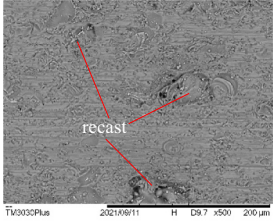
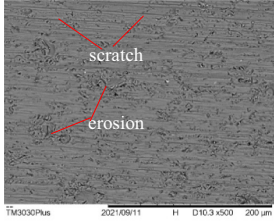
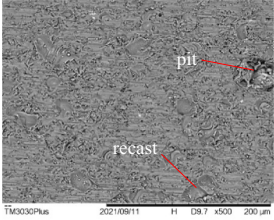
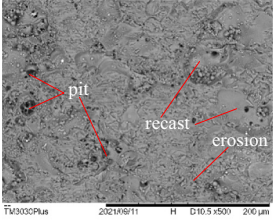
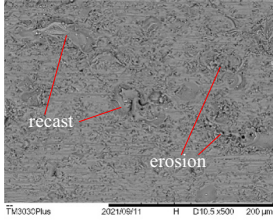
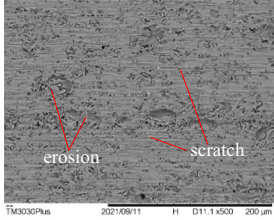


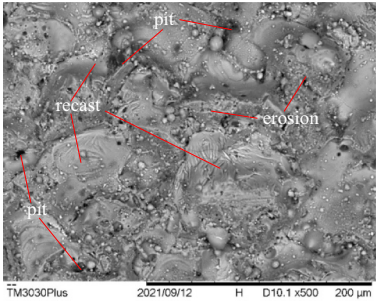
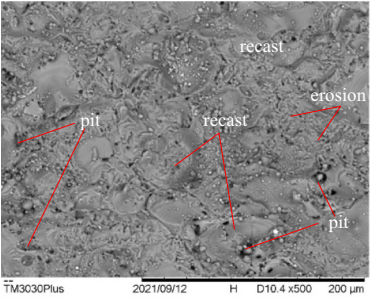
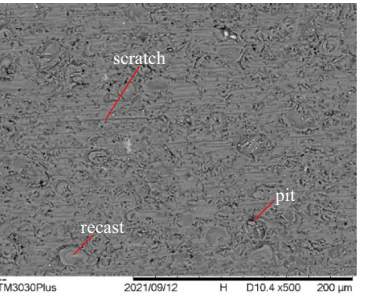
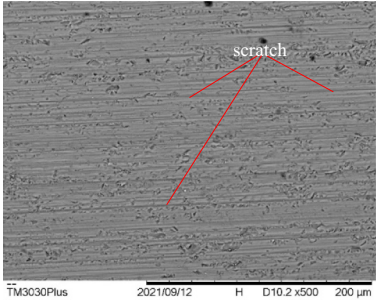
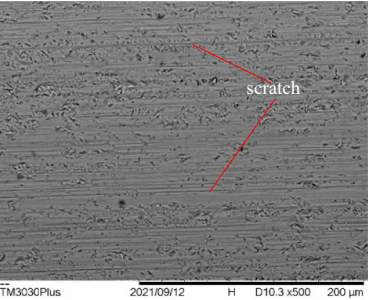
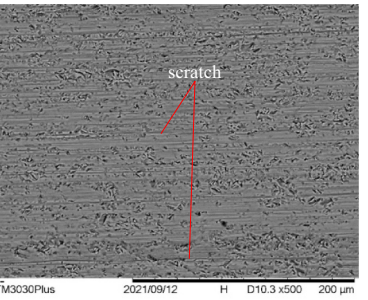
Table 7 Machining accuracy comparison test between DWEDS sawing and DWS sawing using jet cooling

value	60 μm/s, power 3	80 μm/s, power 3	80 μm/s, power 4	70 μm/s, power 5
DWEDS with bath cooling				
DWEDS with jet cooling				

amount after 6 groups of sawing tests with bath cooling under DWEDS and DWS, respectively. It can be seen that the wire wear after processing with DWEDS is slightly higher than that of DWS, and the smoothness of the electrodeposited layer is lower than that of DWS. From the wire diameter, it can be seen that the diameter of diamond wire including abrasive grains in DWS after 6 groups of tests is larger than that of DWEDS, which is 165 μm of

DWS and 160 μm of DWEDS, respectively. The diameters of electroplating layer without abrasive grains have little difference between DWS and DWEDS, corresponding to 144 μm of DWS and 143 μm of DWEDS, respectively. However, more grains of DWEDS wire exposed from the electrodeposited coating than that of DWS wire. It shows that the discharge effect of DWEDS is helpful to the self-sharpening of fixed abrasive wire.

Table 8 Machining accuracy comparison test between DWEDS sawing and DWS sawing using jet cooling

Feed speed	30 μm/s	40 μm/s	50 μm/s
Bath DWEDS			
Bath DWS			

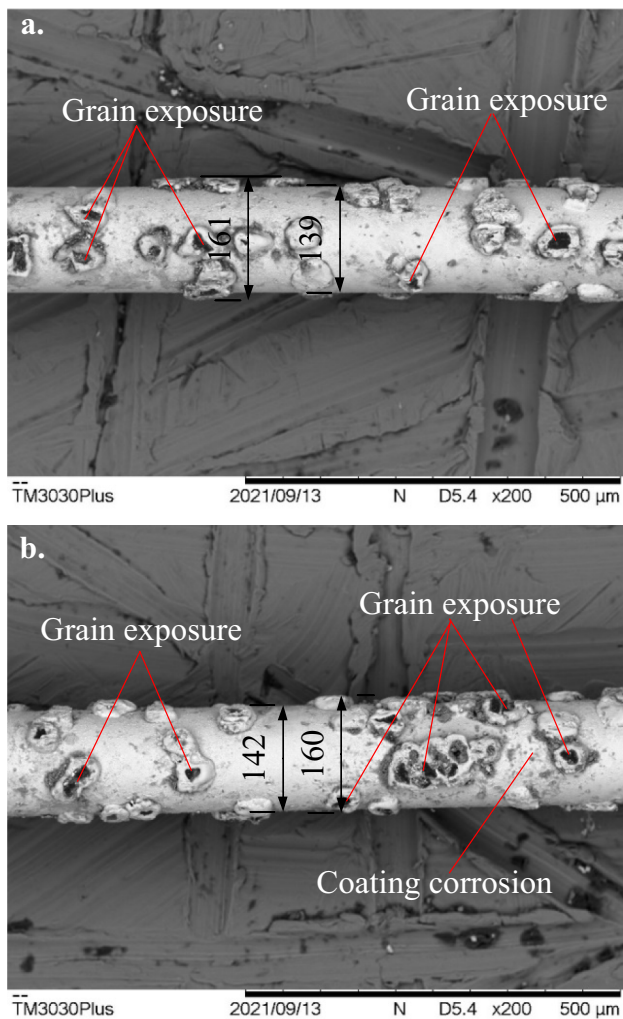


Fig. 17 Wire wear under the same sawing amount of silicon material (a DWEDS under bath cooling; b DWEDS under jet cooling)

5 Conclusion

In this paper, the DWEDS method using bath cooling was studied. Some conclusion can be drawn as follows:

- (1) The machining accuracy in bath cooling is better than that of jet cooling, whether in DWS or in DWEDS. The machining accuracy in DWEDS is better than that in DWS because it improves the macro force and reduces the wire deformation and the resulting wire bow.
- (2) The roughness of bath cooling is better than jet cooling because it improves the cooling and lubrication, but the adverse effect is that chip removal becomes difficult as the fluidity of bath becomes poor. The surface roughness of DWEDS is not as good as DWS as the electrical discharge has etching effect on surface. However, from

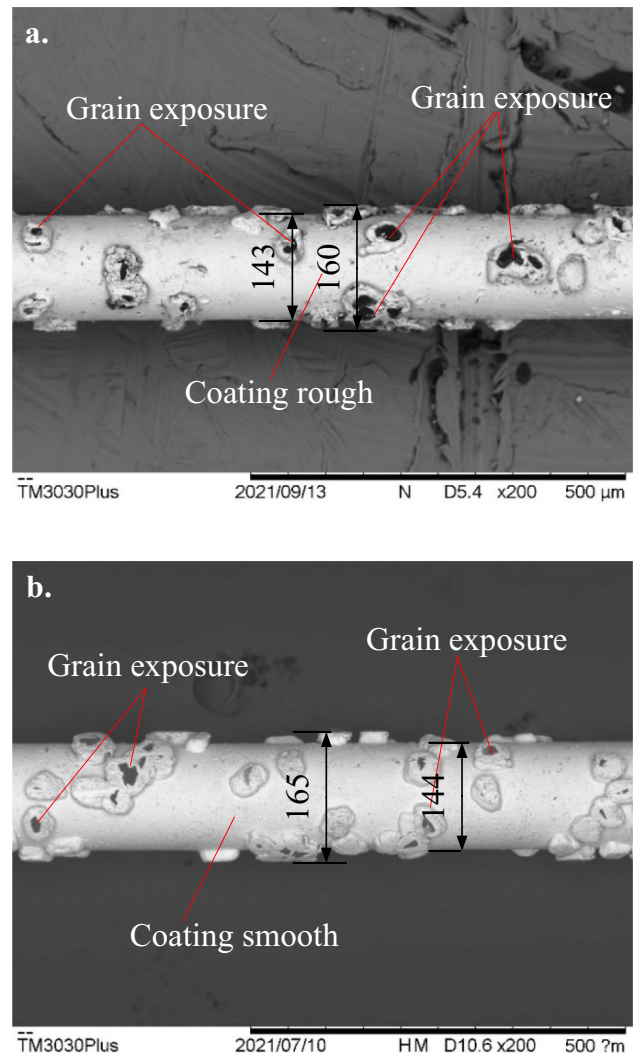


Fig. 18 Wire wear under the same sawing amount of silicon material (a DWEDS; b DWS)

- the surface morphology, the wire mark is significantly improved, the roughness is reduced, and the waviness and other larger scale indicators are improved. The above viewpoint is also proved by the appearance of electron microscope.
- (3) In terms of tension, bath cooling is better than jet cooling in most parameters. The tension stability and tension envelope value obtained by DWEDS using the two cooling methods are better than that of DWS, indicating that the processing state of DWEDS is better.
 - (4) It is known from SEM that the surface with large roughness in DWEDS corresponds to the prominent discharge etching. The electroplated coating wear of diamond wire caused by discharge effect in DWEDS is more serious than in DWS, but it also plays the role of wire self-sharpening.

Author contribution Jian Qiu: conceptualization, methodology, data curation, software, writing — original draft, visualization, validation, program. Xiaofei Li: software. Jianzhuang Lv: validation, equipment. Shanbao Zhang: sample detection and other early research.

Funding This work was supported by National Independent Innovation Demonstration Zone of Shandong Peninsula, Shandong, China.

Availability of data and material All allowed data has been provided in the manuscript.

Code availability Not applicable.

Declarations

Ethics approval This work has no potential conflicts of interest. This work has no research involving human participants and/or animals.

Consent to participate Not applicable.

Consent for publication Not applicable.

Conflict of interest The authors declare no competing interests.

References

- Xiao H, Wang H, Yu N (2019) Evaluation of fixed abrasive diamond wire sawing induced subsurface damage of solar silicon wafers. *J Mater Process Tech* 273:116267
- Kumar A, Kaminski S, Melkote SN, Arcona C (2016) Effect of wear of diamond wire on surface morphology, roughness and subsurface damage of silicon wafers. *Wear* 364–365:163–168
- Cheng K, Luo X, Ward R, Holt R (2003) Modeling and simulation of the tool wear in nanometric cutting. *Wear* 255:1427–1432
- Murthy HGK (2015) Evolution and present status of silicon carbide slurry recovery in silicon wire sawing. *Resour Conserv Recycl* 104:194–205
- Wu H (2016) Wire sawing technology: a state-of-the-art review. *Precis Eng* 43:1–9
- Ozturk S, Aydin L, Celik E (2018) A comprehensive study on slicing processes optimization of silicon ingot for photovoltaic applications. *Sol Energy* 161:109–124
- Yin YK, Gao YF (2020) Experimental study on slicing photovoltaic polycrystalline silicon with diamond wire saw. *Mat Sci Semicon Proc* 106:104779–104779
- Lu Z, Zhang D, Zhang X (2020) Effects of high-pressure coolant on cutting performance of high-speed ultrasonic vibration cutting titanium alloy. *J Mater Process Tech* 279:116584
- Goel S, Luo X, Comley P, Reuben RL, Cox A (2013) Brittle–ductile transition during diamond turning of single crystal silicon carbide. *Int J Mach Tool Manu* 65(2):15–21
- Li C, Piao YC, Hu YX, Wei ZZ, Li LQ, Zhang FH (2021) Modelling and experimental investigation of temperature field during fly-cutting of KDP crystals. *Int J Mech Sci* 210(15):106751
- Liu N, Zou X, Yuan J (2020) Performance evaluation of castor oil-ethanol blended coolant under minimum quantity lubrication turning of difficult-to-machine materials. *J Manuf Process* 58:1–10
- Sales WF, Schoop J, Jawahir IS (2017) Tribological behavior of PCD tools during superfinishing turning of the Ti6Al4V alloy using cryogenic, hybrid and flood as lubri-coolant environments. *Tribol Int* 114:109–120
- Khatri A, Jahan MP (2018) Investigating tool wear mechanisms in machining of Ti-6Al-4V in flood coolant, dry and MQL conditions. *Precis Manu* 26:434–445
- Khanna N, Shah P, Chetan (2020) Comparative analysis of dry, flood, MQL and cryogenic CO₂ techniques during the machining of 15–5-PH SS alloy. *Tribol Int* 146
- Prassan S, Navneet K, Chetan (2020) Comprehensive machining analysis to establish cryogenic LN₂ and LCO₂ as sustainable cooling and lubrication techniques. *Tribol Int* 148:106314
- Ghasemi SE, Ranjbar AA, Hosseini MJ (2017) Forced convective heat transfer of nanofluid as a coolant flowing through a heat sink: Experimental and numerical study. *J Mol Liq* 248:264–270
- Mia M, Dhar NR (2018) Effects of duplex jets high-pressure coolant on machining temperature and machinability of Ti-6Al-4V superalloy. *J Mater Process Tech* 252:688–696
- Rajaguru J, Arunachalam N (2020) A comprehensive investigation on the effect of flood and MQL coolant on the machinability and stress corrosion cracking of super duplex stainless steel. *J Mater Process Tech* 276:116417
- Kaynak Y, Gharibi A, Yilmaz U (2018) A comparison of flood cooling, minimum quantity lubrication and high pressure coolant on machining and surface integrity of titanium Ti-5553 alloy. *J Manuf Process* 34:503–512
- Gueli M, Ma J, Cococetta N, Pearl D, Jahan MP (2021) Experimental investigation into tool wear, cutting forces, and resulting surface finish during dry and flood coolant slot milling of Inconel 718. *Procedia Manuf* 53:236–245
- Race A, Zwierzak I, Secker J (2020) Environmentally sustainable cooling strategies in milling of SA516: effects on surface integrity of dry, flood and MQL machining. *J Clean Prod* 288:125580
- Qiu J, Li X, Zhang S (2021) Research on an improved bath cooling and lubrication method for diamond wire sawing. *The Int J Adv Manuf Tech* 112:2123–2132
- GB, T 6618 (2009) Test method for thickness and total variation of silicon slices. China Stand Press Beijing 2009
- GB, T 6619 (2009) Test method for bow of silicon wafers. China Stand Press Beijing 2009
- GB, T 6620 (2009) Test method for measuring warp on silicon slices by noncontact scanning. China Stand Press Beijing 2009
- ISO 1101 (2017) Geometrical product specifications (GPS) – geometrical tolerancing – tolerances of form, orientation, location and run-out. Int Organ Stand
- ISO 14660–1 (1999) Geometrical Product Specifications (GPS) – geometrical features – part 1: general terms and definitions. Int Organ Stand
- GB, T 29505 (2013) Test method for measuring surface roughness on planar surfaces of silicon wafer. China Stand Press Beijing 2014
- GB, T 30860 (2014) Test methods for surface roughness and saw mark of silicon wafers for solar cells. China Stand Press Beijing 2014
- GB, T 1031 (2009) Geometrical Product Specifications (GPS) – surface texture: profile method - surface roughness parameters and their values. China Stand Press Beijing 2009
- ISO 1302 (2002) Geometrical Product Specifications (GPS) – indication of surface texture in technical product documentation. Int Organ Stand
- ISO 4287 (1997) Geometrical Product Specifications (GPS) – surface texture: profile method – terms, definitions and surface texture parameters. Int Organ Stand

Publisher's Note Springer Nature remains neutral with regard to jurisdictional claims in published maps and institutional affiliations.